

# A novel hybrid control strategy of wind turbine wakes in tandem configuration to improve power production

M.E. Nakhchi, S. Win Naung, M. Rahmati\*

Faculty of Engineering and Environment, Northumbria University, Newcastle upon Tyne NE1 8ST, UK

## ARTICLE INFO

### Keywords:

Wind farm  
Wake control  
Power generation  
Large eddy simulation  
Annual energy production

## ABSTRACT

The wind turbines that operate in the wake region of the upstream turbines produce less power and may suffer serious structural issues due to highly unsteady flows, which can reduce the life expectancy of the turbines. In this study, a novel hybrid wake control strategy for the wind farm power generation enhancement is proposed, which is based on highly accurate large eddy simulations coupled with the actuator line method. The combined effects of yaw angle and tilt angle control methods on the performance improvement of downstream wind turbines in wind farm layouts have not yet been investigated. This work would be the first attempt to evaluate the hybrid wake-control strategy of tandem wind turbines. It is found that the vortex generation is stronger at lower tilt angles because more parts of the rotor are affected by the wakes of the upstream wind turbine. An optimisation analysis is also provided to find the optimum wake deflection angles of the upstream turbine to maximize the electrical power generation. The results show that an accumulative power production increment of 17.1% is achieved by controlling both yaw angle ( $\theta = 30^\circ$ ), and tilt angle ( $\varphi = 24^\circ$ ). The power obtained in the present study is approximately 6.1% higher than previous wake control techniques. By using the hybrid control strategy, an annual energy production enhancement of 3.7% is achieved, which is higher than the previous wake-controlled wind farm layouts.

## 1. Introduction

To face global warming challenges, wind farms, as a reliable source of renewable energy, have attracted major interest in reducing greenhouse gas emissions. To generate electricity, wind turbines are usually arranged to create a wind farm in one location to reduce the total costs of wind energy power production. The wind turbine wake reduces the wind speed and increases the flow disturbance and vorticities for the second and third layers of the wind farm layout. Therefore, the wind turbines that operate in the wake region of the upstream turbines can produce significantly less power. Adaramola and Krogstad [1] experimentally investigated the effect of upstream wake on electrical energy production of the wind turbines and concluded that the power generation could reduce up to 46% compared to the wind turbines operating in ideal wind conditions. The wind farm layouts and turbine blades are commonly optimised [2] with different methods to improve the overall performance and power generation of a wind plant.

As mentioned above, there are usually several wind turbines assembled in a wind farm to deliver a huge amount of electrical power and reduce the maintaining costs and power transmission equipment. If

the wind turbines are installed in uncontrolled configuration, then the wakes generated from the upstream turbine would significantly reduce the power generation of the downstream turbines and increase the fluctuating forces on the turbine blades, which decrease the life length of the wind turbines due to blades fatigue. Several studies have been focused on proposing wake control methods of offshore wind farms [3]. There are several analytical studies for wake control analysis, including low, medium and high-fidelity methods. Most of the analytical methods to model the wind turbines wake are low-fidelity methods such as three-dimensional wake models [4], and wake control methods based on the Gaussian distribution for the velocity deficit [5]. High-fidelity numerical methods are necessary to capture the transient flow structure, power generation fluctuations, and other essential parameters of wind turbines with time.

The Reynolds-averaged Navier-Stokes (RANS) models have been extensively used to predict aerodynamic and structural characteristics of horizontal-axis and vertical-axis wind turbines [6]. However, because of the complex structure of turbulent vorticities in the wake region of the turbines, it is essential to use high-fidelity models to capture the instantaneous variations of power generation and wake profile of the turbines in a wind farm layout. Several numerical studies have been

\* Corresponding author.

E-mail address: [mohammad.rahmati@northumbria.ac.uk](mailto:mohammad.rahmati@northumbria.ac.uk) (M. Rahmati).

<https://doi.org/10.1016/j.enconman.2022.115575>

Received 17 January 2022; Received in revised form 31 March 2022; Accepted 1 April 2022

Available online 13 April 2022

0196-8904/© 2022 The Authors. Published by Elsevier Ltd. This is an open access article under the CC BY license (<http://creativecommons.org/licenses/by/4.0/>).

Nomenclature			
$c$	Chord length	$\delta$	Distance between actuator points
$C_D$	Drag coefficient	$\Delta$	Averaged grid size
$C_L$	Lift coefficient	$\epsilon$	Smearing factor
$C_s$	Smagorinsky constant parameter	$\theta$	Yaw angle
$D$	Rotor diameter	$\nu$	viscosity
$F$	Force	$\rho$	Air density
$N$	Grid size	$\tau_{ij}^{SGS}$	Sub-grid scale stress
$P$	Power	$\varphi$	Tilt angle
$St$	Strouhal number	$\Omega$	Rotational speed
$\tilde{S}_{ij}$	Resolved strain level in the tensor form	<i>Subscripts</i>	
$TSR$	Tip speed ratio	cyl	Cylinder
$U$	Flow velocity	in	Inlet
<i>Greek letters</i>		n	normal
$\alpha$	Angle of attack	rel	Relative
$\beta$	Rotor cone angle	sgs	Sub-grid scale
$\gamma$	Pitch angle	t	Tangential
		$\infty$	Freestream

carried out in the past decade to simulate the transient wake structure of the wind farms, such as the large eddy simulation (LES) of Nilson et al. [7] and Calaf et al. [8].

To accurately predict the aerodynamic forces and power generation of the wind turbines, different numerical methods are proposed by researchers, such as the nonlinear frequency domain method [9], or spectral/hp element method [10]. However, these methods require significant computation time. Other computational methods have been developed to predict the power generation and wake structure of wind farms, such as the actuator disk method (ADM) [11], and the actuator line method (ALM) [12]. Zhang and Zhao [13] used the ALM method to simulate a wind farm wake based on the deep learning method. They found that the proposed method could calculate the unsteady wakes of a three-by-three wind farm layout. Some other numerical methods, such as Parallelized LES Model (PALM) [14] method, are also utilized to compare the results of ALM and ADM methods in wind farms based on large-eddy simulations [15]. The additional advancement of wind farm simulators is still an active area like the ExaWind solver proposed by Sprague et al. [16].

Although highly accurate numerical models can capture the details of flow structure and wake generation of wind turbines, they require long and heavy simulations and huge computation resources to model a realistic wind farm layout equipped with several wind turbines with different geometrical parameters such as various yaw angles. Mache et al. [17] numerically investigated the wake structure of two wind turbines in tandem alignment by Weather Research and Forecasting (WRF)-LES method. They found that turbulent flow becomes more consistent after the second wind turbine. Recently, Bartholomew et al. [18] developed a powerful open-source code to simulate high-fidelity wind farm layouts more efficiently than the previous open-source and commercial wind farm solvers. This solver is based on a newly proposed ALM-LES method and provides the possibility to analyse various single-control or hybrid-control strategies of turbine wakes. The details of the ALM method to simulate wind turbine wakes is discussed by Jha et al. [19]. The ALM-LES method can also measure the wake profile of multi-turbine wind farms with a yaw control strategy [20].

The effects of wind turbine wake depend on the distance between wind turbines and wake control strategy. The distance between the wind turbine clusters in a wind farm depends on several design limitations. Due to additional power transmission costs between long-distance wind turbines, it is essential to use optimum wake deflection methods to reduce the unfavourable wake effects as much as possible. Using an optimized wake control strategy will help to maximise the total power

generation of a wind farm layout without increasing the manufacturing costs. There are six different wake control strategies in the previous studies, including: a) yaw misalignment control [21], b) blade pitch control [22], c) tilt angle control [23], d) torque control [24], and e) cone angle control [25]. Yang et al. [26] used LES to investigate the wake deflection of a wind farm in complex terrain. They concluded that the yaw control strategy is essential to the enhancement of the total power generation of the wind farm, and more detailed studies are necessary to find the best wake control strategy for wind turbines. Wang et al. [27] compared analytical, numerical and experimental models to control the wind turbine wake using pitch control strategy. Their study revealed that using a pitch angle of  $7^\circ$  did not add any noticeable influence on wake deflection. It is also discussed by Nash et al. [25] that pitch control strategy does not seem very practical in real wind farm models. Comparable to pitch control, the torque control method does not lead to a major increment in structural loads. However, it doesn't seem to increase the power production of two wind turbines in tandem configuration [25]. Changing the upside turbine's tilt angle can enhance the overall power production of tandem turbines configuration with a specific distance between wind turbines. In the numerical study of Weipao et al. [28], the authors tested different wake control strategies to maximize the total power generation of a wind farm and found that using a tilt angle of  $15^\circ$  for the upstream National Renewable Energy Laboratory (NREL) 5 MW wind turbine can enhance the total power generation by 12.0%. It was concluded that controlling the tilt angle is more efficient than pitch and torque control strategies. Moreno et al. [29] performed multi-objective optimization on a wind farm layout to control the wake effects at different wind speeds. They found that the optimized layout produced more energy with fewer costs.

Among the wake deflection methods, yaw-angle control and tilt-angle control play important roles in the power generation enhancement of wind farms. However, due to the wind turbine design limitations, it is not possible to use wind turbines with yaw angles of higher than  $30^\circ$ , and negative tilt angles. This means that there is an optimized design point to maximise the power generation of wind turbines without increasing the unwanted additional structural loads on the wind turbine blades. To the authors' knowledge, there are no numerical or experimental studies to investigate the combined effects of yaw angles and tilt angles control methods to maximize the energy production of a wind farm. Therefore, the main novelty of this study is to fill the knowledge gap in the design of wind farms by proposing a new hybrid wake control strategy, to benefit from the advantages of both yaw-control and wake-control methods and to avoid the additional structural loads.

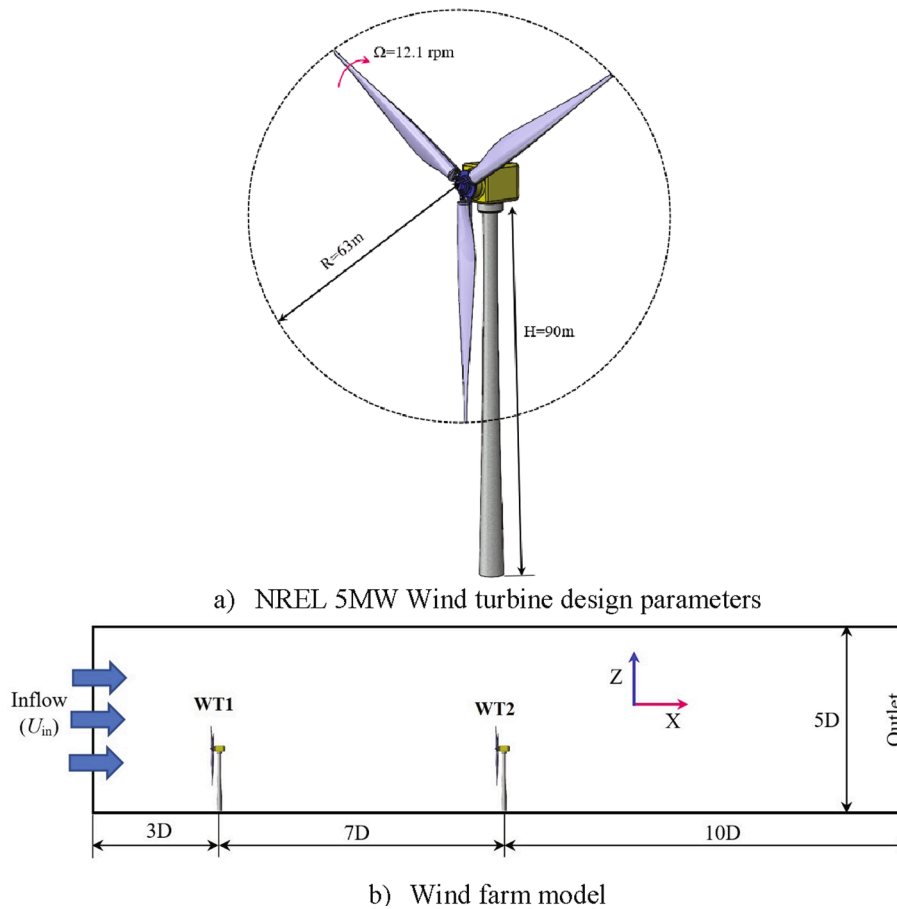


Fig. 1. Schematic view of the wind turbine design parameters and tandem array configuration.

### 1.1. Research hypothesis and objectives

The central hypothesis of this paper is that an efficient hybrid wake control strategy of the design parameters is required, based on an accurate prediction of aerodynamic loads and a detailed wake analysis, to optimise the overall power generation of wind turbines in arrays in a wind farm. The physical description of the NREL 5 MW wind turbine, yaw/tilt angles, and other design parameters are described in section 2. The governing equations of the ALM-LES method, which is employed to investigate the effects of hybrid yaw-tilt angles control strategy on the power generation of two wind turbines in tandem configuration, and mesh details are presented in section 3. The main results of wake profiles and isosurface contours on vorticity in both controlled and uncontrolled wind farm layouts are provided in section 4. The main objective of this study is to maximise the power output of the downstream wind turbine by proposing a hybrid wake deflection method for the upstream wind turbine. The details of the optimisation analysis are provided in section 5. An overall discussion of the main findings of this study and conclusions are summarised in sections 6 and 7.

## 2. Physical description

Fig. 1 shows the computational domain used in the present numerical study. The wind farm contains two NREL 5 MW wind turbines in tandem configuration. The computational domain is  $20D$  in the  $x$ -direction,  $5D$  in the  $y$ -direction, and  $5D$  in the  $z$ -direction ( $D = 126$  m is the wind turbine rotor diameter). The first wind turbine (WT1) is located at  $3D$  distance after the inflow, and the second wind turbine (WT2) is located at a distance of  $7D$  in the downstream direction of WT1 in the  $x$ -direction. The distance between the tandem wind turbines ( $7D$ ) is

Table 1

Main design parameters of the tandem wind turbines.

Parameter	Value	Unit
Rated power ( $P_{out}$ )	5	MW
Rated wind speed ( $U_{rated}$ )	11.4	m/s
Tip-speed ratio (TSR)	7.0	–
Rotor diameter ( $D$ )	126.0	m
Rotation speed ( $\Omega$ )	12.1	rpm
Number of blades	3	–
Inflow velocity ( $U_{in}$ )	11.4 ~ 15.0	m/s
Hub height	90	m
Hub diameter	3	m
Rotor cone angle ( $\beta$ )	2.5	°
Yaw angle ( $\theta$ )	–30 ~ 30	°
Tilt angle ( $\varphi$ )	0 ~ 40	°

selected equal to the conventional distance between NREL 5 MW wind turbines [30] for validation purposes. The distance between wind turbines can be determined by considering both accumulative power generation and construction costs. The design parameters of the three-dimensional wind turbines used in the present ALM-LES study are provided in Table 1. The main variables of the present study to control the wake deflection of the upstream wind turbine are the yaw angle ( $\theta$ ) and tilt angle ( $\varphi$ ). The yaw/tilt angles of the downstream wind turbine remain zero because there are no further turbines in the wake region of the last row of wind turbines.

Uniform inflow is imposed at the inlet, while an opening flow condition with zero gradient is imposed at the outlet. On the sidewalls, symmetric boundary conditions are used, and no-slip boundary condition is used on the turbine blades and tower. The definition of these parameters is provided in Fig. 2. It was discussed in the recent review

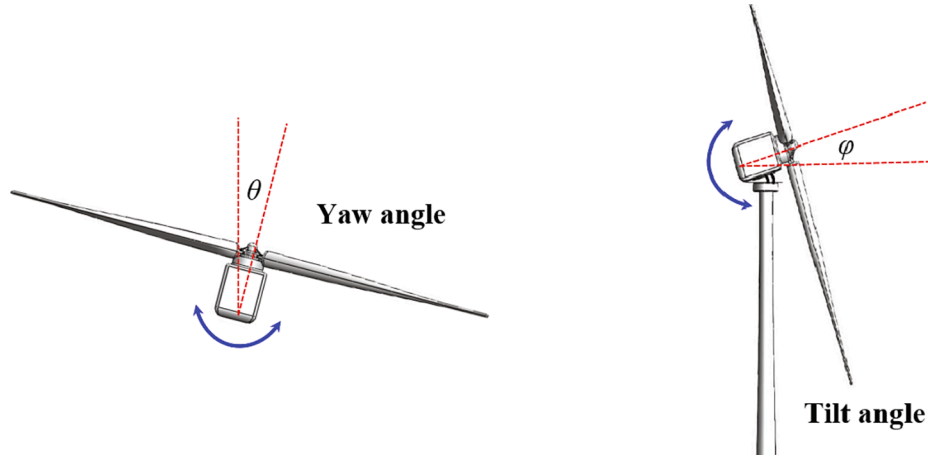


Fig 2. Definition of yaw angle and tilt angle of horizontal-axis wind turbines.

study of Nash et al. [25] that the yaw angle could have positive and negative values. But the tilt angle could only have a positive value to avoid collision of the blades with the wind turbine tower. Therefore, the yaw angle and tilt angle of the upstream wind turbine are selected in the range of  $(-30^\circ \leq \theta \leq 30^\circ)$ , and  $(0^\circ \leq \varphi \leq 40^\circ)$ , respectively. These ranges are popular in the design of wind turbines to avoid collision of blades with the tower and additional fatigue forces on the blades at higher yaw/tilt angles as thoroughly discussed in Ref. [25].

### 3. Governing equations

The Xcompact3D solver is a novel open-source code that is written in Fortran language to solve various incompressible flows [31]. This solver is a high-fidelity, fast, and efficient code to model complex wind farm layouts and also other complex aerodynamic problems. The remarkable properties of the solver, using high-order spectral methods, and powerful parallel computing options, enables us to model a wind farm layout using high-performance computing systems with  $10^4$  or even higher CPU cores. The solver provides all essential parameters of a wind farm, including the output power, blades tangential and normal forces, angle of attack, lift and drag coefficient, thrust forces, and generator torque of each individual wind turbine in a wind-farm layout using various wake-control techniques, such as yaw-controlled and tilt-controlled strategies [31].

The Xcompact3D solver has the option to use LES method to solve unsteady and incompressible turbulent flows. The fluid speed at the tip

of the wind turbine blade doesn't surpass  $\text{Mach} = 0.3$ . In this method, the large-scale eddies are resolved, and a sub-grid scale (SGS) scheme will be used to capture the small-scale eddies [32]:

$$\frac{\partial \tilde{u}_i}{\partial x_i} = 0 \tag{1}$$

$$\frac{\partial \tilde{u}_i}{\partial t} + \tilde{u}_j \frac{\partial \tilde{u}_i}{\partial x_j} = -\frac{1}{\rho} \frac{\partial \tilde{p}}{\partial x_i} + \nu \frac{\partial}{\partial x_j} \left( \frac{\partial \tilde{u}_i}{\partial x_j} \right) - \frac{\partial \tau_{ij}^{SGS}}{\partial x_j} + f_i \tag{2}$$

where  $u$  is the inflow velocity,  $p$  is pressure,  $\nu$  is the kinematic viscosity of airflow. It is assumed that turbulence is homogeneous and isotropic [33]. In the above equation, “ $\sim$ ” means that the parameter is resolved.  $f_i$  is the source term, and  $\tau_{ij}^{SGS} = \tilde{u}_i \tilde{u}_j - \tilde{u}_i \tilde{u}_j$  is the sub-grid scale stress. Various LES methods are available in the Xcompact3D solver. In the present work, the well-known Smagorinsky model is selected for the transient turbulent flow simulations. Based on this model, the deviant part of the sub-grid scale stress term in the Navier-Stokes equation can be estimated by [32]:

$$\tau_{ij}^{SGS.dev} = \tau_{ij}^{SGS} - \frac{1}{3} \tau_{kk}^{SGS} \delta_{ij} \approx -2\nu_{SGS} \tilde{S}_{ij} \tag{3}$$

In Eq. 3,  $\nu_{SGS}$  is the sub-grid scale viscosity, and  $\tilde{S}_{ij} = \frac{1}{2} \left( \frac{\partial \tilde{u}_i}{\partial x_j} + \frac{\partial \tilde{u}_j}{\partial x_i} \right)$  is the resolved strain level in the tensor form. The SGS viscosity can be expressed as a function of geometrically averaged grid size ( $\Delta$ ) by using

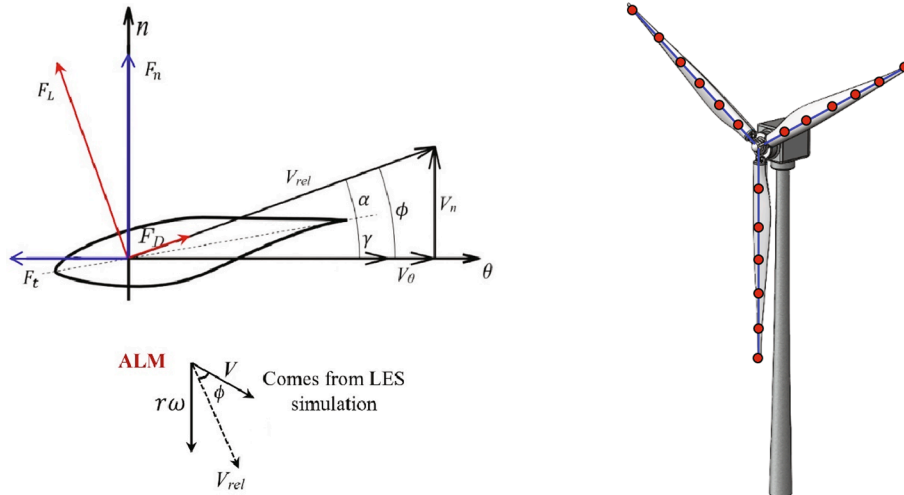


Fig. 3. Actuator line schematic with forces imposed on wind turbine blade section.

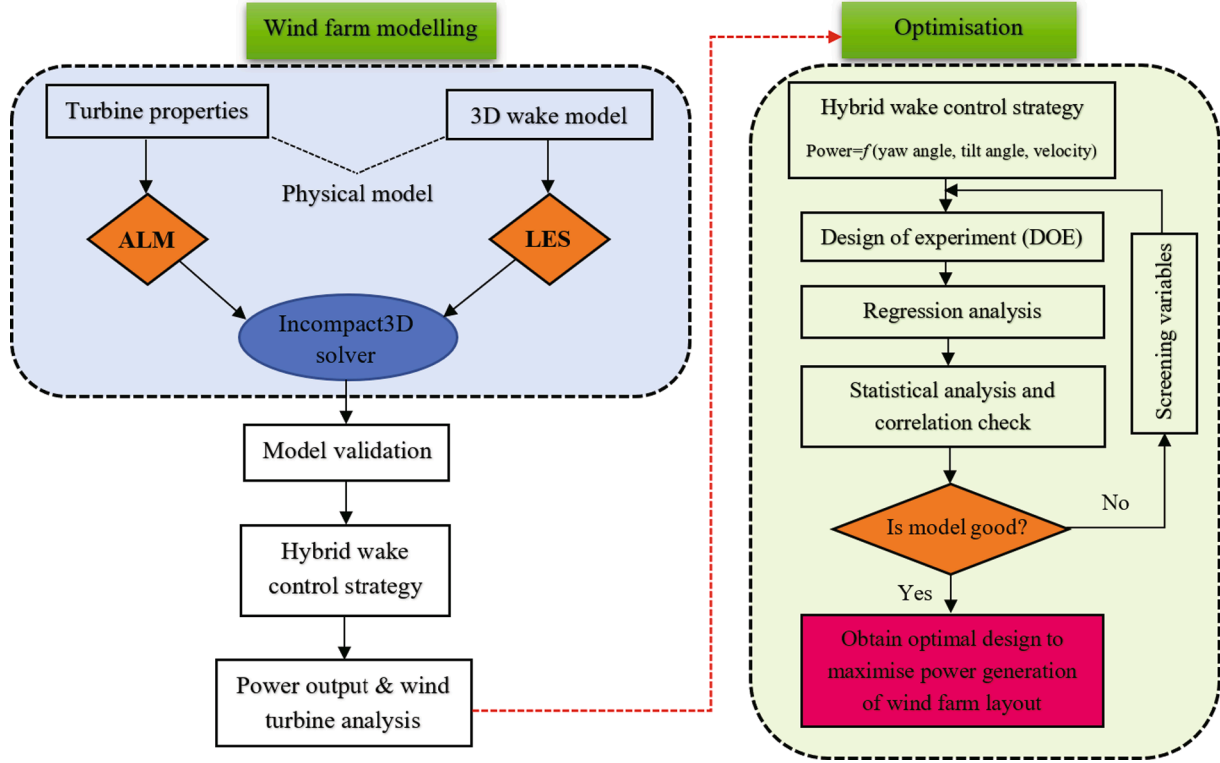


Fig. 4. Wind farm solver and optimisation flowchart.

Prandtl's mixing length principle as [32]:

$$\nu_{SGS} = (C_s \Delta)^2 \left| \tilde{S}_{ij} \right| \quad (4)$$

In the above equation the  $\Delta = \sqrt[3]{\Delta_1 \Delta_2 \Delta_3}$  in the cartesian coordinates, and  $C_s$  is the Smagorinsky constant parameter. The rate of the resolved strain tensor can be calculated by  $\left| \tilde{S}_{ij} \right| = \sqrt{2 \tilde{S}_{ij} \tilde{S}_{ij}}$ . The Smagorinsky constant parameter ( $C_s$ ) is kept constant at 0.168 in the present LES study to simulate turbulent flow over two wind turbines in tandem format.

### 3.1. Actuator line method

The actuator line method [34] replaces wind turbine blades by a line of body force elements rotating in the turbulent fluid flow. This method combines the Navier-Stokes solver (such as the LES method explained in Section 3.1) with forces distributed alongside actuator lines. The details of forces on the cross-section view of the NREL-5 MW wind turbine blade are shown in Fig. 3. In this figure,  $\omega$  is the angular velocity,  $V_n$  and  $V_\theta$  are the normal and tangential velocities on the wind turbine airfoil, and  $\gamma$  is the pitch angle of the blade,  $\phi = \text{atan}\left(\frac{V_n}{r\omega - V_\theta}\right)$  is the fluid angle, and  $\alpha = \phi - \gamma$  is the angle of attack of the wind turbine airfoil at each cross-section. At every actuator element point, the relative fluid velocity ( $V_{rel}$ ) can be calculated as a function of tangential and normal velocities as through the neighbouring cells [12]:

$$V_{rel} = \sqrt{V_n^2 + V_t^2}, V_t = r\omega - V_\theta \quad (5)$$

The actuator line method uses the fluid information at each time step and computes the drag and lift forces ( $F_D, F_L$ ) on the surface of the blade by using these equations [12]:

$$F_L = \frac{1}{2} \rho V_{rel.c} C_L \quad (6)$$

$$F_D = \frac{1}{2} \rho V_{rel.c} C_D \quad (7)$$

where  $c$  is the local chord length of the wind turbine blade at each section,  $\rho$  is air density and  $C_L$  and  $C_D$  are drag and lift coefficient, respectively. The drag and lift forces can be divided into their components in the normal ( $F_n$ ) and tangential ( $F_t$ ) directions as:

$$F_n = F_L \cos \phi + F_D \sin \phi, F_t = F_L \sin \phi - F_D \cos \phi \quad (8)$$

These forces are multiplied by the space between the actuator points toward the blade tip direction to compute the aerodynamic forces on each wind turbine blade. The aerodynamic forces on the blade can be summarized in vector form as [30]:

$$f = \frac{F}{\epsilon^2 \pi^{3/2}} e^{-\left(\frac{r}{\epsilon}\right)^2} \quad (9)$$

where  $r$  is the distance from the actuator points to nodes where  $f$  will be projected to, and  $\epsilon$  is the smearing factor that controls the distribution of the body force gradient. Several empirical equations have been proposed to compute this smearing factor as functions of the element size, blade chord length and rotor diameter. As discussed by Churchfield et al. [35], a factor of 0.035 can be used when a standard elliptical force distribution is employed relative to the wind turbine blade diameter. To make the ALM-LES simulations stable, it is suggested by Qian et al. [36] to select the smearing factor ( $\epsilon$ ) as  $\epsilon = \max\left[\frac{c}{5}, 2\Delta\right]$ . The same assumption is used in the present numerical analysis to ensure the stability of the simulations.

The wind turbine tower can be modelled with the same actuator-line method discussed above. The tower can be replaced by the corresponding body forces over the cylindrical structure of the tower. The lift and drag coefficient on the tower can be computed by [36]:

$$C_{L,tower} = A \sin(2\pi f t), C_{D,tower} = 1.2 \quad (10)$$

where  $f$  is the vortex shedding frequency and can be computed by

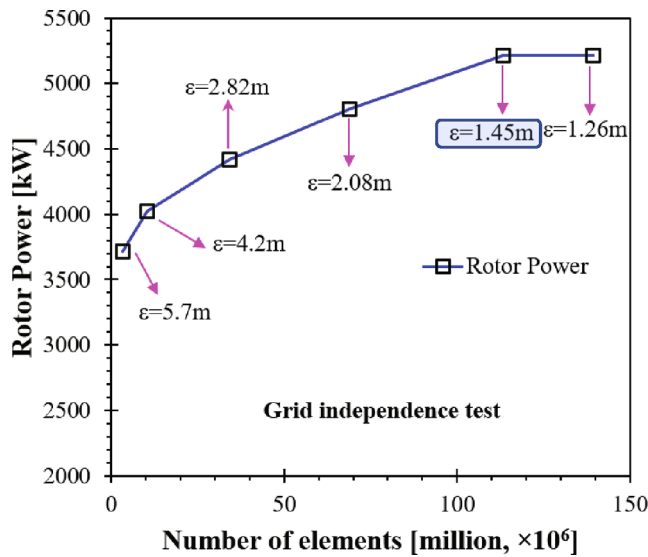


Fig. 5. Grid independence study of NREL 5 MW wind turbine.

Table 2  
Computation time and deviation of the output power for different mesh cases.

Number of grids	Computation time (min)	Output power (kW)	Deviation, % $\left(\frac{f_{i+1} - f_i}{f_i}\right) \times 100$
$3.420 \times 10^6$	14.1	3715.1	
$1.037 \times 10^7$	67.0	4025.8	8.34
$3.418 \times 10^7$	104.8	4417.0	9.73
$6.882 \times 10^7$	155.1	4805.2	8.78
$1.132 \times 10^8$	198.3	5210.3	8.42
$1.394 \times 10^8$	245.5	5210.5	0.01

Strouhal number ( $St = fD_{cyl}/U_{\infty}$ ).

As discussed earlier, there are several numerical and analytical wind turbine wake models in the literature. In the present study, the actuator line method (ALM) coupled with large eddy simulations (LES) based on a powerful and accurate CFD solver is employed for the numerical simulations of two wind turbine wakes in tandem configuration. Fig. 4 shows the simulation flowchart of the wind farm based on the ALM-LES method and optimisation algorithm used in the present study to find the optimum wake-deflection hybrid control method. The optimisations are performed with statistical analysis to predict the power production as a

function of yaw angle, tilt angle and inflow velocity. The details of the optimisation process will be discussed in section 5.

Fig. 5 shows the grid independence study to find the most appropriate mesh size for the numerical simulations over two wind turbines in tandem configuration. Six different element sizes ( $1.26 \leq \epsilon \leq 5.7m$ ) were selected for the present study. The results show that by increasing the number of elements from  $3.42 \times 10^6$  to  $6.88 \times 10^7$ , the power output of a single uncontrolled NREL 5 MW wind turbine increased significantly. However, the power output of  $\epsilon = 1.45m$  (corresponds to  $N = 113.25 \times 10^6$ ) is less than 0.1% compared to  $\epsilon = 1.26m$ . Therefore, the mesh resolution of  $\epsilon = 1.45m$  can accurately predict the power generation of the wind turbine (5 MW), and it is selected for the ALM-LES simulations.

A comparative study is performed to investigate the effects of mesh refinement on computation time and deviations of the output power obtained at each step of the mesh refinement is Table 2. The simulations are performed on 1024 CPU cores with 64 Gb of memory on a super-computer. It can be seen that for  $N = 1.132 \times 10^8$  the deviation for the output power is less than 0.1%, and the computational time is 198.3 min.

#### 4. Results and discussion

Before performing an in-depth analysis involving two wind turbines, a simulation of a single wind turbine model is first conducted and compared to well-known reference numerical data available in the literature. Fig. 6 (a) shows the comparison of the tangential force per unit length with respect to the blade radius between the present simulation, the fully resolved mesh (FRM) solution [37], and the ALM method [32]. As seen, an excellent agreement is obtained between the FRM analysis and the present simulation, and the results are also reasonably comparable to the reference simulation. It is seen that the tip loss is accurately captured in the simulation as the force is nearly zero at the blade tip, and it is in good agreement with the experiment. The dimensionless wake profile ( $U/U_{ref}$ ) is also computed at one rotor diameter downstream of the wind turbine in the present simulation, and it is compared to the fully resolved LES numerical model [38] and the actuator line method [12]. This comparison is provided in Fig. 6(b). The fluctuations in the profiles that can be clearly observed are directly associated with the effects of the tower and the nacelle of the wind turbine. The streamwise velocity is reduced up to 90% of the reference or the freestream velocity. Overall, the results obtained from different numerical models agree well, and the results from the present simulation are close to that of the fully resolved LES model.

Fig. 7 provides the instantaneous velocity contours extracted in the meridional view to show the development of the downstream flow and

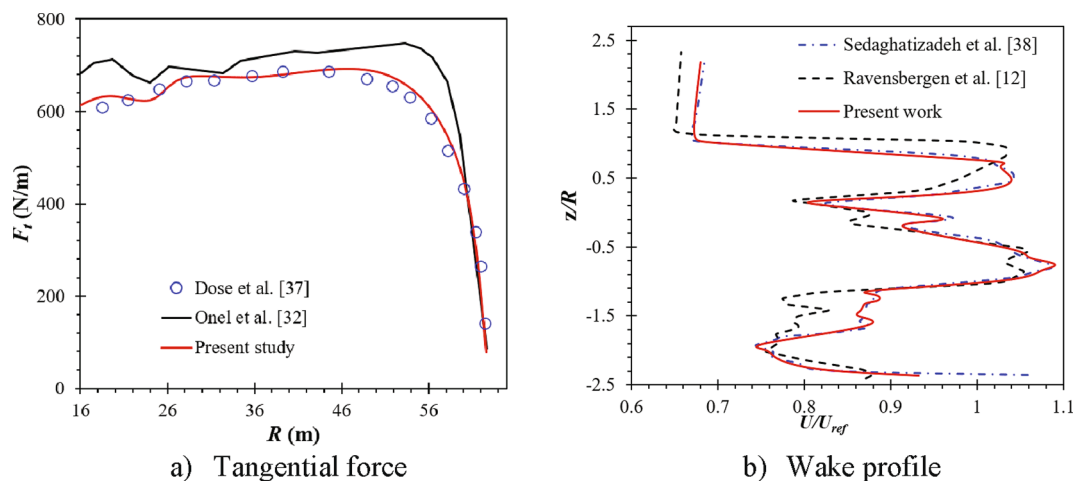


Fig. 6. Validation of the proposed ALM-LES model with previous experimental and numerical studies.

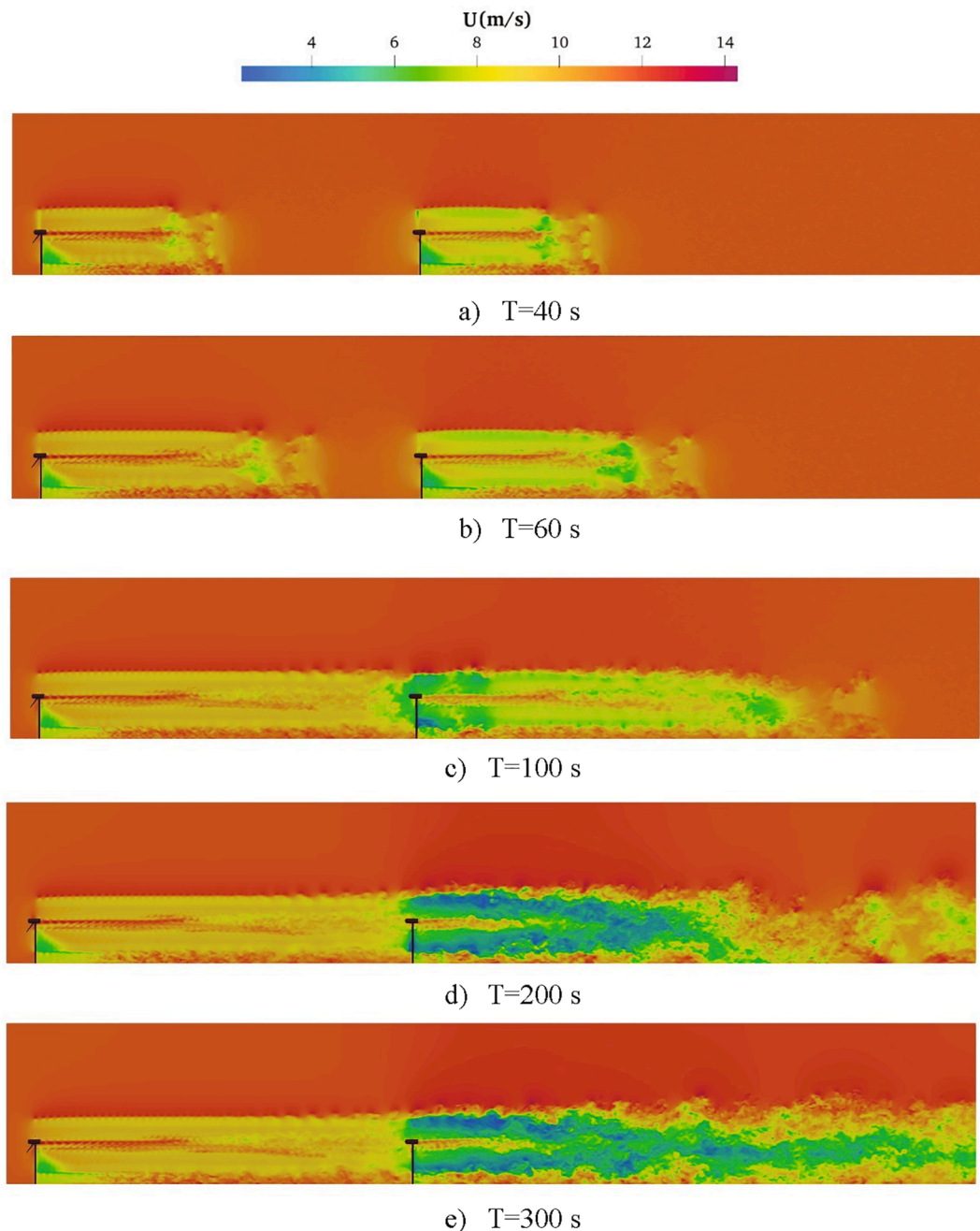


Fig. 7. Variations of instantaneous velocity contours over two uncontrolled tandem wind turbines at  $\theta = \varphi = 0^\circ$ ,  $TSR = 7.0$  and  $U_{in} = 11.4$  m/s.

wake from each turbine and the effect of flow structures from the upstream turbine on the downstream one. The wind turbines are indicated by black colour in the contours. Within the initial periods, the same pattern of the downstream wake is developed from both turbines due to a uniform inflow with the same wind speed. After one minute, the downstream wind turbine starts to gradually experience the effects from the upstream turbine as the flow from the upstream turbine approaches the downstream turbine. Once it reaches the downstream turbine, a significant impact can be clearly observed. The wake structures from the upstream turbine not only hit the downstream one but also mix with those generated from the downstream turbine. This interaction results in a stronger wake generation behind the downstream wind turbine. After 200 s, the velocity field around the downstream turbine is significantly reduced, with the wake becoming stronger in the downstream region. As time goes on, the downstream turbine is completely overwhelmed by the flow from the upstream turbine. The wake and turbulence behind the

downstream turbine are amplified by those of the upside turbine. However, the velocity field behind it is much weaker than the upstream turbine due to disturbed inflow with a smaller magnitude.

The effects of title angle  $\varphi$  on the development of vorticity structures are presented in Fig. 8. In this analysis, the yaw angle is kept at  $0^\circ$  for both wind turbines, and only the tilt angle for the upstream turbine is varied, whilst the tilt angle for the downstream turbine is also kept at  $0^\circ$ . When the tilt angle of both turbines is  $0^\circ$ , the tip vortex structures generated from each turbine are in line with each other. The downstream turbine possesses stronger vortex generation due to the impact from the upstream turbine and the mixing of wake structures. Changing the tilt angle of the upstream turbine to  $20^\circ$  causes some of the wake structures to pass over the upper part of the rotor of the downstream turbine, while the lower part is more affected by the wakes. This behaviour of interaction leads to the wake expansion behind the downstream wind turbine being slighter larger than that of the  $0^\circ$  tilt

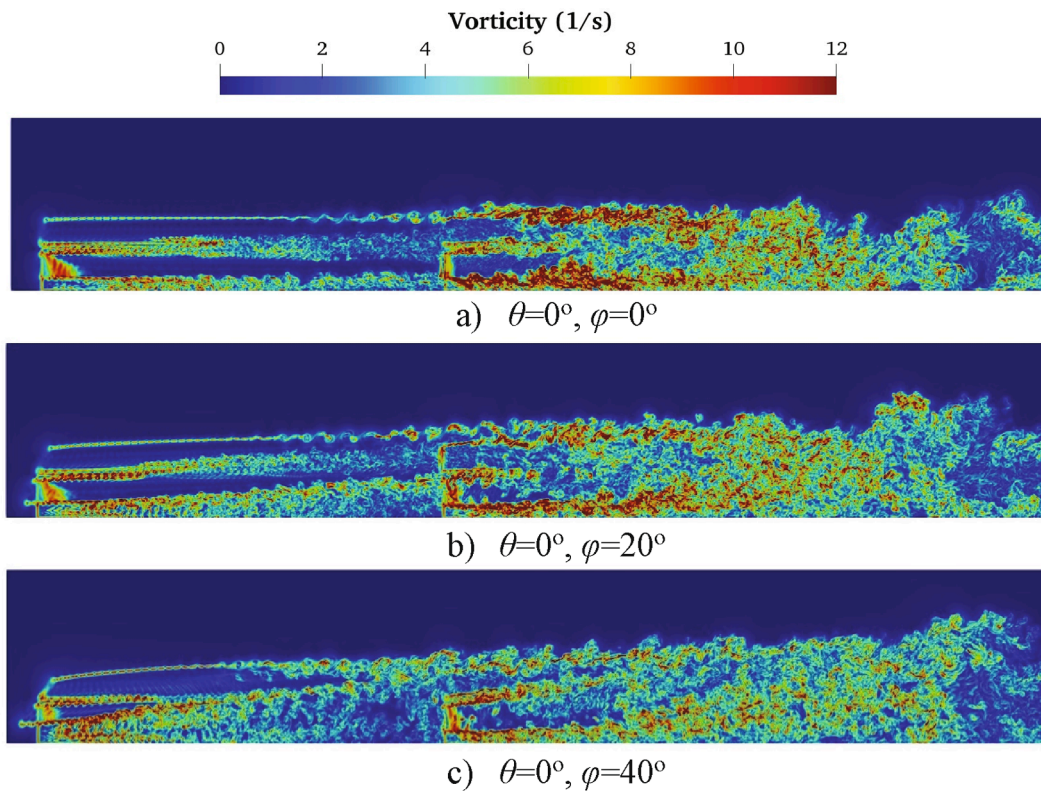


Fig. 8. Instantaneous vorticity contours in the mid-rotor plane for different tilt-controlled layouts.

angle case. Increasing the tilt angle further to  $40^\circ$  results in more flow passing over the upper part of the rotor of the downstream wind turbine, which, in turn, causes the wake expansion in an inclined upward direction.

Fig. 9 demonstrates the effect of variation of yaw angle of the upstream wind turbine on the downstream one. A total of 5 cases are discussed in this figure. The effects of both positive and negative angles are investigated. In addition, the combined effect of yaw angle and tilt angle is also analysed in this study. The standard case in which the yaw and tilt angles are set to  $0^\circ$  for both wind turbines is also added to highlight the effects when changing these angles. The performance of a wind turbine is dependent on the behaviour of the freestream flow and the presence of neighbouring wind turbines in a wind farm. As discussed, the downstream wind turbine is significantly influenced by the wake and turbulence created from the upstream wind turbine. When the yaw angle of the upstream wind turbine is set to  $15^\circ$ , the tip vorticity and wake structures generated from the upstream wind turbine is carried through the freestream velocity. Consequently, the wake structures behind the downstream turbine are slightly deformed compared to the uncontrolled wake position ( $\theta = 0^\circ$ ,  $\varphi = 0^\circ$ ). This behaviour is enlarged by increasing the yaw angle of the upstream turbine to  $30^\circ$ . A twist in the advection and diffusion of the vortex structures behind the upstream turbine is clearly observed in this case. The deflection of the wake behind the downstream turbine is more apparent at this yaw angle.

An interesting behaviour is observed when the yaw angle and tilt angle of the upstream turbine are simultaneously changed. Due to the non-zero yaw angle of the upstream turbine, the downstream wind turbine is partially affected by the wake of the upstream turbine. Moreover, the tilt angle helps some of the flow and wake structures pass

over the upper part of the downstream wind turbine. Therefore, it is expected that the performance of the downstream wind turbine is to be increased compared to the standard case when the two turbines are in line with each other. The wake generation is also not as strong as the standard case; however, the wake expansion seems to be larger.

The behaviour of the flow by shifting the yaw angle of the upstream wind turbine is presented in Fig. 10, which shows the contours of axial velocity at the hub height. As discussed, the velocity field behind the downstream wind turbine is much smaller than that of the upstream turbine. In the case of  $0^\circ$  yaw angle, the downstream turbine is entirely in the wake of the upstream turbine, leading to a stronger vortex generation due to the mixing of vortex structures from both turbines. Shifting the yaw of the upstream wind turbine from the direction of the incoming wind by a certain degree while the downstream turbine is facing the wind leads to the loss of kinetic energy captured by the upstream turbine. However, it could also reduce the effect on the downstream wind turbine as the rotor is only partially affected by the wakes of the upstream wind turbine. Rotating the yaw of the upstream wind turbine either in the positive or negative direction when the downstream turbine is facing the wind does not produce noticeable effects as the wake generation seems to be identical with an opposite direction. The results show that by increasing the distance between the wind turbines from 5D to 9D, the wake generation is decreased noticeably. However, as mentioned earlier, increasing the distance among wind turbines in a wind farm will increase the power transmission and maintenance costs. Therefore, it is recommended to use the distance of 7D among NREL-5 MW wind turbines in complex layouts.

The effect on the development of vorticity structures and flow behaviour when the tilt angle of the upstream wind turbine is changed is

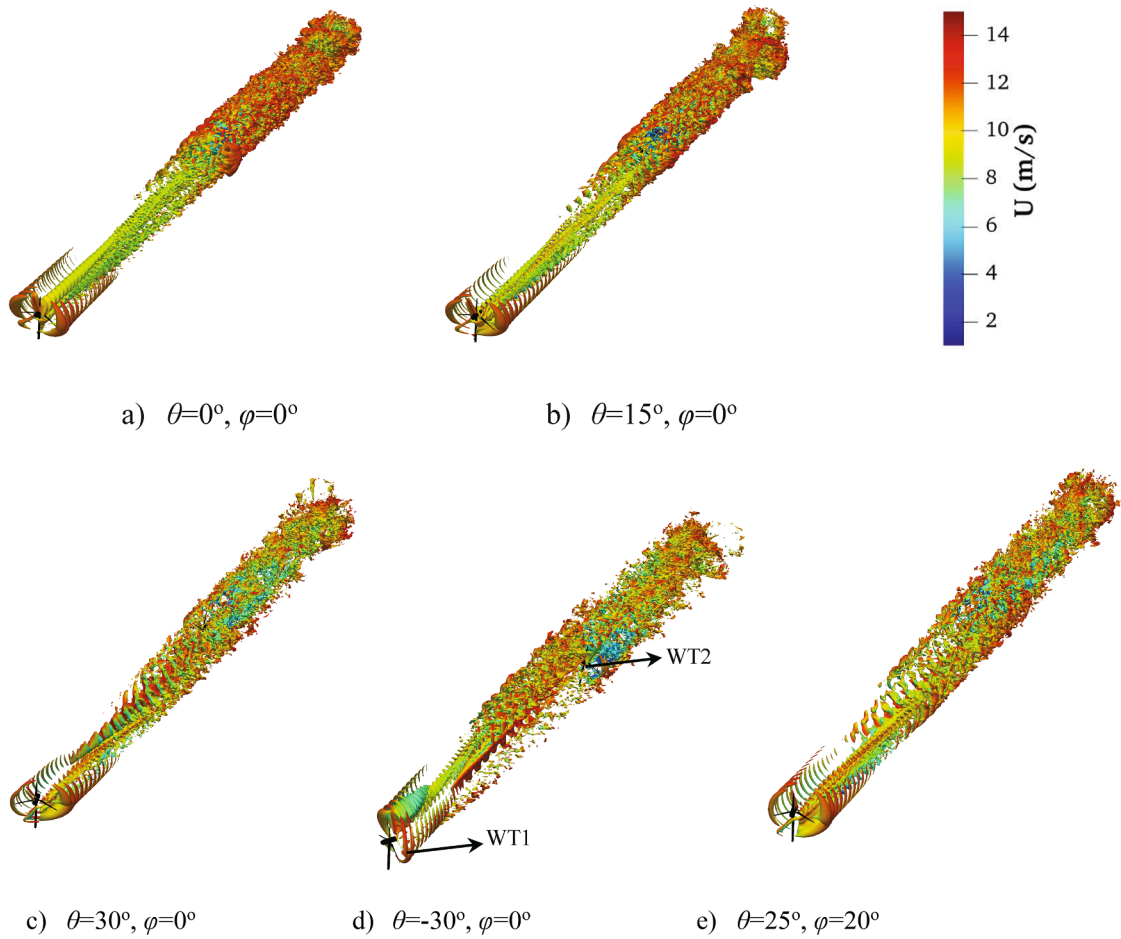


Fig. 9. Isosurface contours of axial velocity over two tandem wind turbines with different wake control conditions.

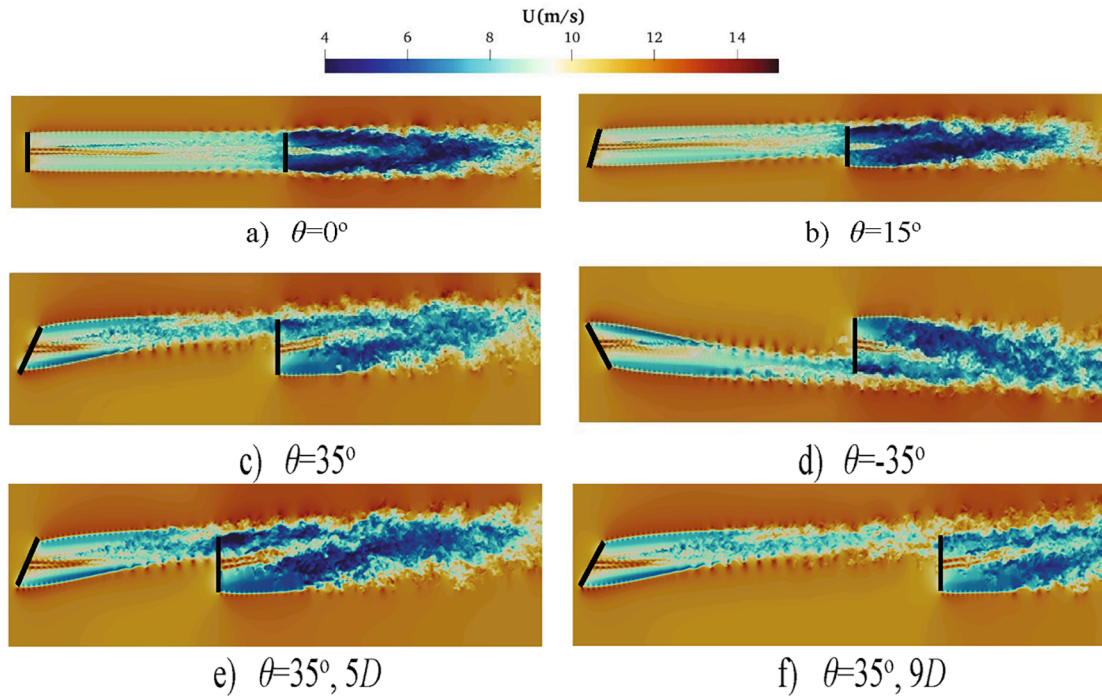


Fig. 10. Hub height axial velocity contours for different yaw angles and distances between the wind turbines.

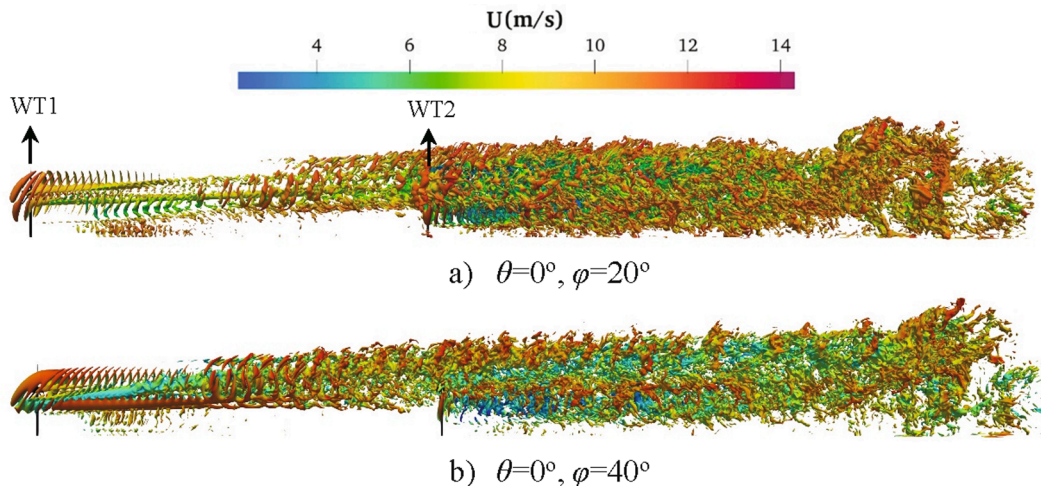


Fig. 11. The effects of tilt angle ( $\varphi$ ) on vorticity generation of two wind turbine arrays.

illustrated in Fig. 11. The tilt angle of the upstream wind turbine is  $20^\circ$  and  $40^\circ$  while that of the downstream wind turbine is set to  $0^\circ$ . It is seen that the behaviour of the vortex generation near the downstream wind turbine is similar when the tilt angle is present. However, the vortex generation is stronger at a lower tilt angle because more parts of the rotor is influenced by the upstream wind turbine wake. The wake interaction and mixing of the flow structures from both turbines cause a stronger vortex generation. On the other hand, at a greater tilt angle, the flow structures from the upstream turbine overpass the rotor of the downstream turbine, and therefore, the power loss due to the interaction with the wakes can be reduced.

Cross-section views of the streamwise velocity distributions around upstream and downstream wind turbines at different axial locations are shown in Fig. 12. The effects of the yaw and tilt angles on the wake behaviour are highlighted by investigating different cases which consider yaw angle, tilt angle or both yaw and tilt angles of the upstream turbine. At uncontrolled conditions ( $\theta = 0^\circ$ ,  $\varphi = 0^\circ$ ), the wake development is dominated by the generation of tip vorticity. The advection of swirl flow is established by the freestream flow and the rotation of the rotor. The wake expansion is initiated as it diffuses into the air. In this case, the wake expansion can be observed around the rotor rotation with no deflection behind both turbines.

When the tilt angle of the upstream wind turbine is changed, the wake deflection can be observed behind the turbine. It is observed that the wake expansion and deflection move towards the upward direction. On the other hand, changing only the yaw angle of the upstream wind turbine shifts the direction of the wakes towards the side, and the wakes partially interact with the rotor of the downstream wind turbine. This behaviour of the interaction leads to the wake behind the downstream turbine being deflected towards the side. The combined effects of the hybrid yaw and tilt angle control strategy are shown at  $\theta = 20^\circ$  and  $\varphi = 20^\circ$ . Modifying the yaw angle of the upstream turbine caused the advection of the swirl flow to be twisted before interacting with the downstream turbine. The tilt angle deviation forces some of the flow to pass over the rotor of the downstream turbine. As a result, the wake deflection tends to occur both in the upwards and side directions. Consequently, the most significant wake deflection is occurred by using the newly proposed hybrid wake control strategy, which helps improve the power generation of the downstream wind turbines in a wind farm layout.

The dimensionless downstream wake profiles, normalised by the mean streamwise velocity, computed at different axial locations are presented in Fig. 13. The effect of different control strategies such as changing only yaw angle or both yaw and tilt angles on the wake profiles are investigated. The effects of the nacelle and the tower on the wakes are clearly observed within the rotor diameter. Setting a positive yaw angle for the upstream wind turbine shifts the profiles to the positive  $y/D$  direction. At  $X = 2D$ , the fluctuations due to the nacelle and the tower occur around the centre of the rotor rotation. The wake deflection due to the yaw and tilt angle change can be identified as it goes further downstream. At  $X = 5D$ , the largest wake deflection is observed when both yaw angle and tilt angles are controlled. It is seen that the effects of yaw and tilt angles are reduced in far wakes at  $X = 9D$  and  $X = 12D$ . The effects of the nacelle and the tower also gradually decrease as it goes far away from the turbine. The minimum peaks in the wake profiles are found at  $2D$  behind each wind turbine and at  $X = 9D$  when no yaw and tilt angles are changed.

#### 4.1. Computational cost

All simulations are performed on ARCHER2 UK national supercomputer. The overall computation efficiency of the present model is shown in Fig. 14. The CPU times are normalised with the time required for 32 cores. Using 2048 and 4096 CPU cores don't provide the best computation efficiency for the present study. Therefore, using 1024 CPU cores on 8 nodes can provide the best computation efficiency, and the computation time is around 148 min for the wind farm in tandem configuration.

## 5. Optimization

One of the objectives of this numerical work is to find the optimum design points of the wake-controlled wind farm to maximize power generation. The Response Surface Methodology (RSM) is a powerful and accurate statistical method for the performance optimisation of wind turbines. This method provides the ability to propose a second-order polynomial correlation to predict the power production of wind farms as a function of the design parameters. In the present analysis, MINITAB software with face-centred configuration is used for optimisation purposes. As discussed earlier in Fig. 4, the power generation of the hybrid

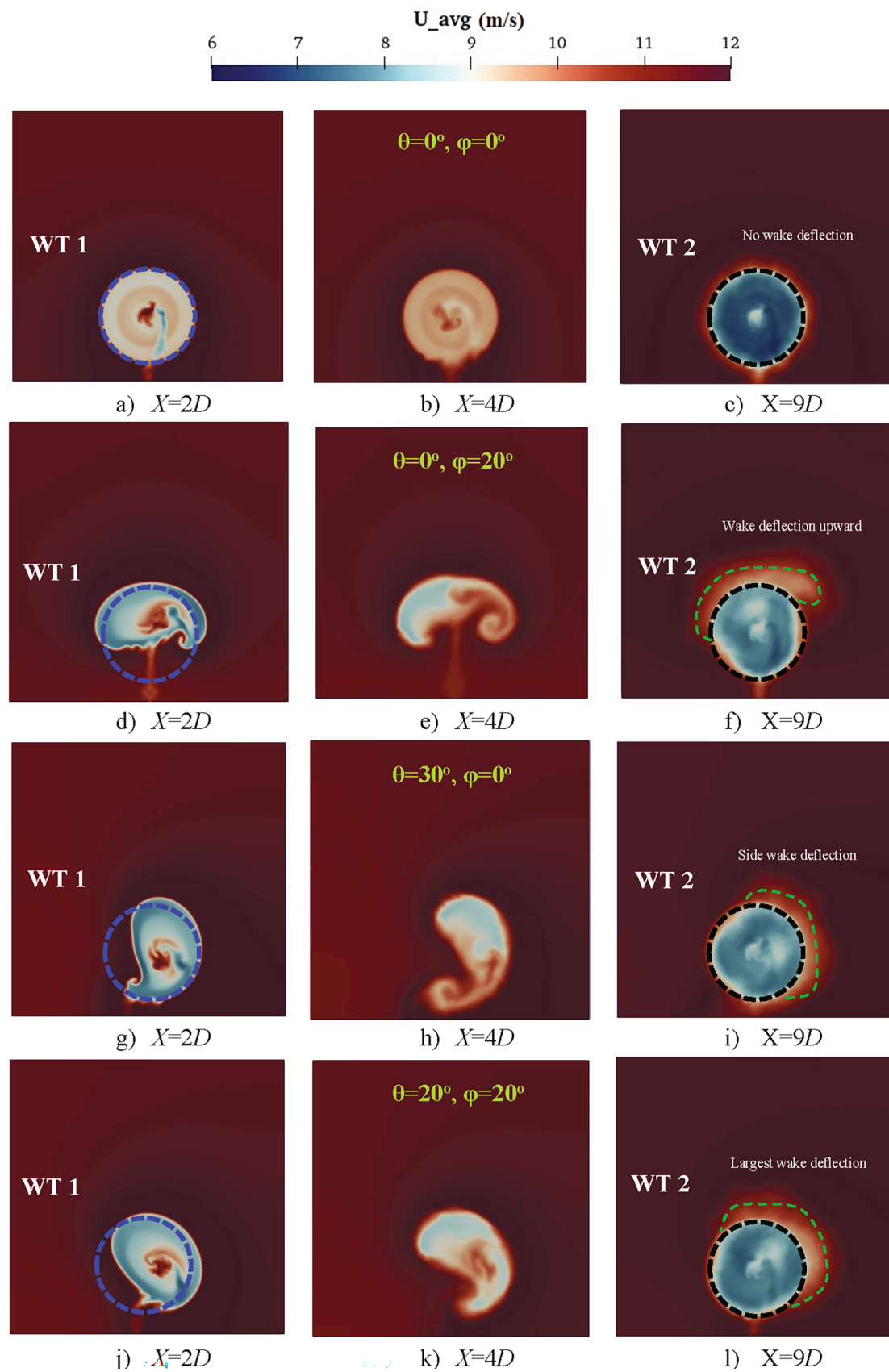


Fig. 12. Contours of the normalized mean streamwise velocity on the cross-stream y-z plane at wake positions  $X = 2D, 4D$  and  $9D$ .

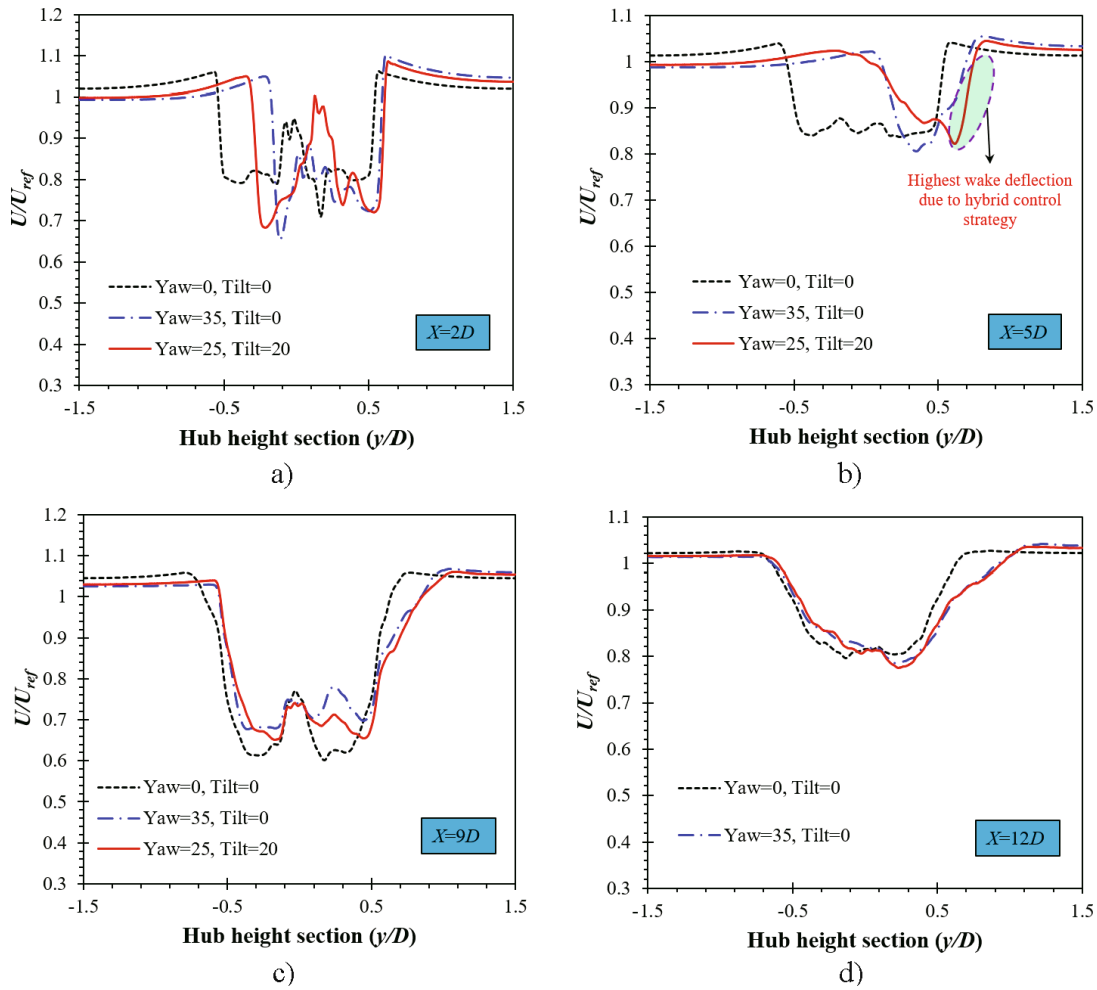


Fig. 13. Profiles of the normalized mean streamwise velocity in the wake of two inline wind turbines at  $X = 2D, 5D, 9D,$  and  $12D$ .

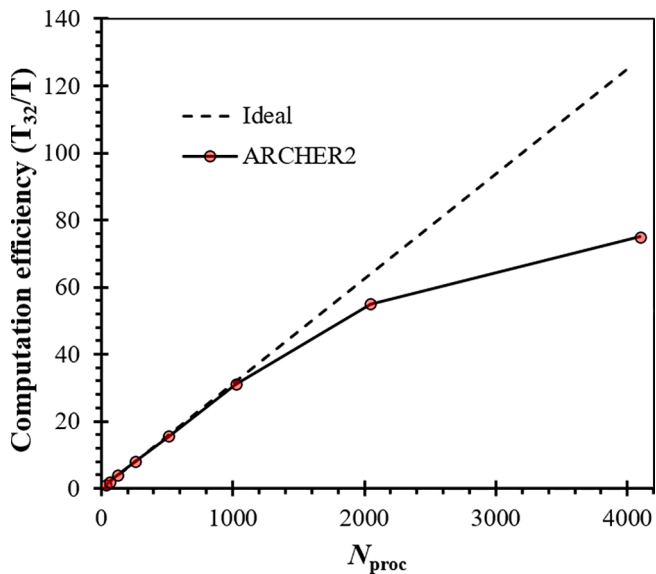


Fig. 14. Computation efficiency of the present study on ARCHER2 cluster.

Table 3  
Wind farm optimization design parameters.

Parameter	Level 1	Level 2	Level 3
$U_{in}$ (m/s)	11.4	13.2	15
Tilt angle ( $\varphi$ )	0	20	40
Yaw angle ( $\theta$ )	-30	0	30

Table 4  
Analysis of variance (ANOVA) for power generation of two wind turbine arrays.

Source	Adj. Sum of squares	DOF	f-value	p-value
A- $U^*$	1.93	1	15.67	0.0027
B- $\theta^*$	0.0029	1	0.0235	0.8812
C- $\varphi^*$	0.6605	1	5.37	0.0430
AB	0.0006	1	0.0050	0.9451
AC	0.0465	1	0.3781	0.5523
BC	0.0066	1	0.0538	0.8213
A <sup>2</sup>	0.0923	1	0.7502	0.4067
B <sup>2</sup>	1.48	1	12.02	0.0061
C <sup>2</sup>	0.7064	1	5.74	0.0376
Model	4.80	9	4.34	0.0158

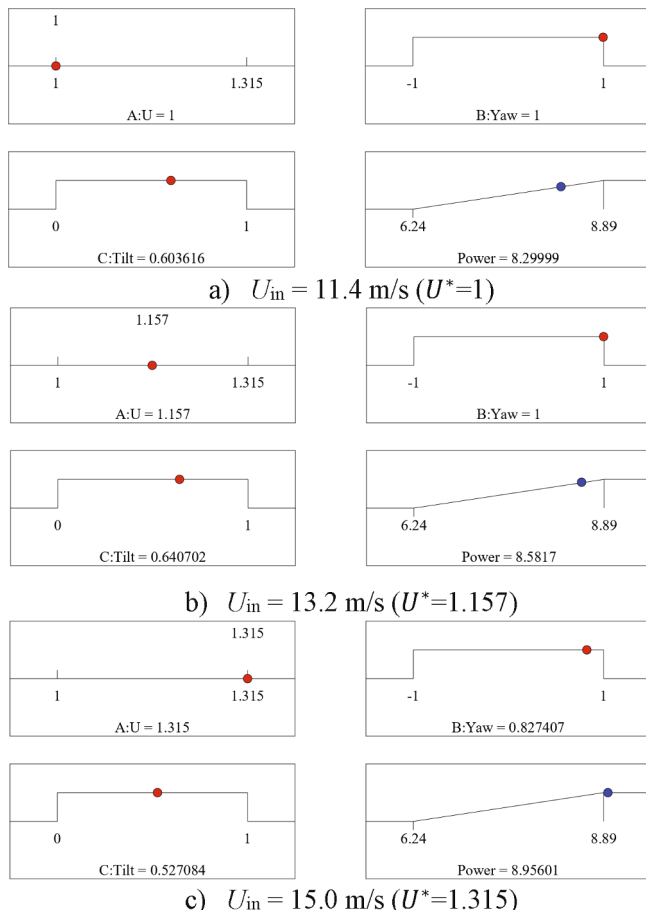


Fig. 15. Optimisation criteria for different inflow velocities.

the present optimisation study are provided in Table 4. The adjusted sum of squares, Degree of freedom (DOF), F-value and P-values of the statistical analysis are provided for different source terms. Each source term is linked to a coded value (A, B, and C) and product of these parameters ( $A \times B$ ,  $A \times C$  and  $B \times C$ ). The p values smaller than 0.05 implies that those source terms have a substantial impact on the power generation of the wind farm. It can be observed that the inflow velocity has the most influence on the power production rate. Moreover, it is observed that tilt angle has more influence on wind farm power generation than yaw-angle control strategy. This finding indicates that more studies should be done on the effects of tilt-angle wake deflection on the output enhancement of complex wind farm layouts.

Based on the optimization results, the optimum yaw angle and tilt angles are predicted at three different inflow velocities in Fig. 15. It is observed that for all tested cases, the highest power output can be achieved at the yaw angle of  $30^\circ$  ( $\theta^* = 1$ ). However, the optimum tilt angle varies with the inflow velocity. This finding indicates that the tilt angle wake-control strategy should be sensitive to the inflow wind speed, and it should be increased at higher air velocities to maximize the power generation in a wind farm layout. The results show that the highest electrical power of 8.95 MW can be obtained from two NREL 5 MW wind turbines with a hybrid wake-control strategy at an inflow velocity of 15 m/s, which is slightly higher than the rated velocity of the wind turbine design. The surface contour plots of the power generation as functions of the design parameters (inflow speed, yaw angle and tilt angle) are presented in Fig. 16. It is observed that the power generation is increased significantly at higher wind speeds, which is physically correct. Moreover, the hybrid effects of yaw-control and tilt-control methods on power production of the wind turbines indicate that the output power of the wind farm can be significantly improved compared to uncontrolled wind farm layout. It is observed that the highest output electrical power can be obtained at  $\theta = 30^\circ$  and  $\phi = 24^\circ$  at rated inflow speed.

Based on the statistical analysis, the following polynomial correlation is proposed to predict the accumulative power generation of two tandem wind turbines as a function of dimensionless design parameters:

$$Power = 0.439U^* + 0.017\theta^* + 0.257\phi^* + 0.0087U^*\theta^* + 0.0762U^*\phi^* + 0.0287\theta^*\phi^* + 0.1832U^{*2} + 0.7332\theta^{*2} - 0.5068\phi^{*2} \quad (11)$$

controlled NREL 5 MW wind turbines can be computed as a function of inflow velocity, tilt angle and yaw angle. The objective is to maximize the overall power generation of a wind farm layout as a function of yaw angle, tilt angle and inflow velocity in a wind farm layout with tandem configuration. The objective function can be expressed as:

$$Power = function(\phi, \theta, U_{in}) \quad (11)$$

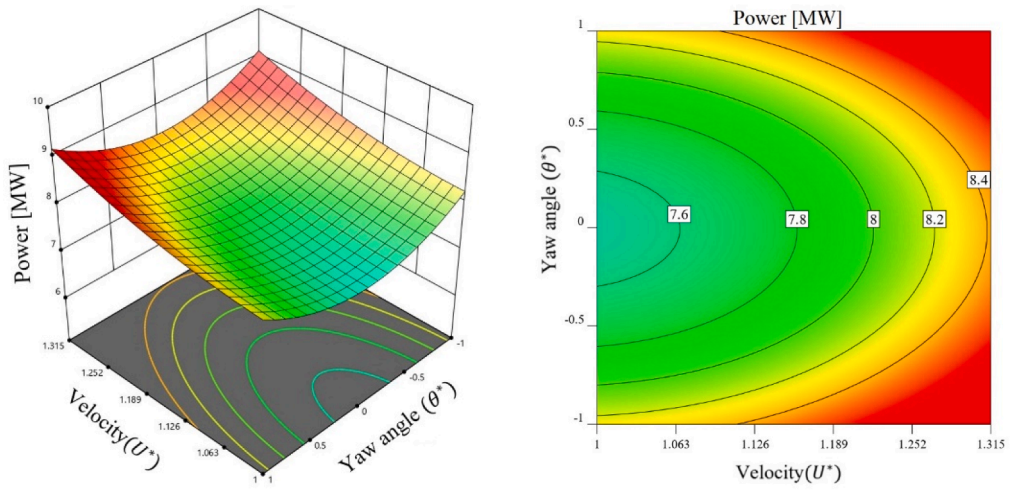
The yaw angle and tilt angle of the upstream wind turbine are selected in the range of  $(-30^\circ \leq \theta \leq 30^\circ)$ , and  $(0^\circ \leq \phi \leq 40^\circ)$ , respectively. The inflow velocity is in the range of  $11.4 \leq U_{in} \leq 15.0$  m/s. Table 3 shows the three different levels selected for the design parameters. Based on the wind turbine design limitations, the tilt angle cannot have negative values to avoid collision between the blades and the tower. The rated inflow velocity for NREL-5 MW wind turbine is 11.4 m/s. Therefore, the first level is selected as the rated velocity. For the third level, the highest inflow velocity used in this study, and level 2 is between these two levels.

Based on the consents of the RSM method, 31 numerical analyses are required as inputs. Regression analysis of the numerical results is performed. To make the present numerical results more general and reproducible, dimensionless forms of the input parameters ( $\theta^* = \theta/30$ ), Tilt angle ( $\phi^* = \phi/40$ ), Velocity ( $U^* = U_{in}/11.4$ ), are employed for the regression analysis. The results of the analysis of variance (ANOVA) for

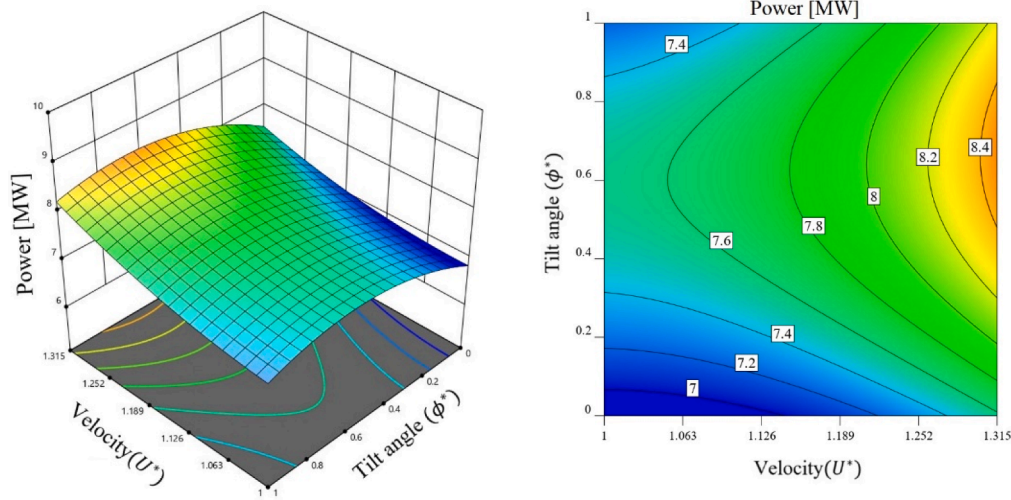
This correlation can predict the power generation of a wind farm for yaw/tilt angles and inflow velocity in the ranges previously mentioned in Table 3. A statistical test is provided in Fig. 17 to show the precision and accuracy of the optimization method (RSM). It can be seen that the predicted power data by Eq. (11) are in agreement with the numerical results.

### 5.1. Energy production analysis

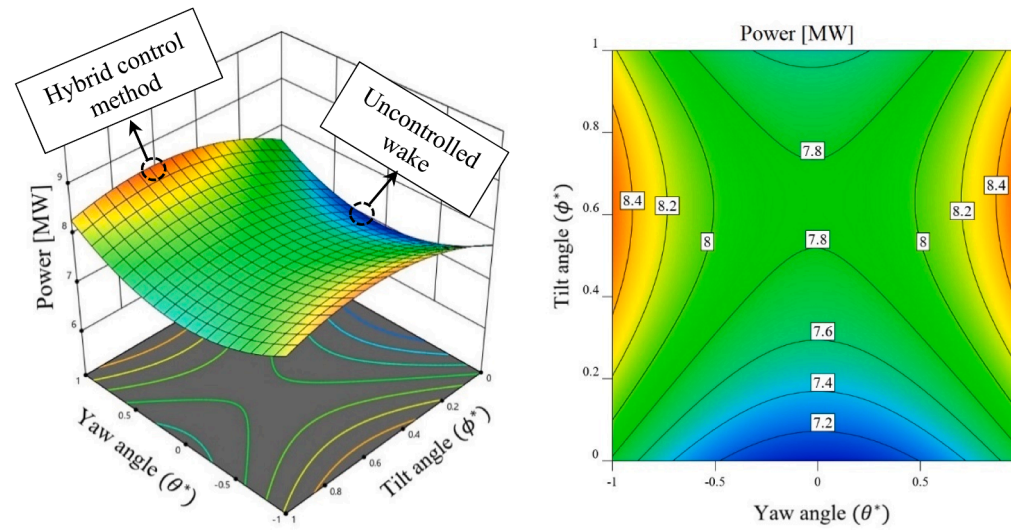
The power production based on different control strategies is analysed in this section. The power production obtained from the present study is compared to those available in the literature [39–42] using different control methods, and they are presented in Fig. 18. It is found that the control of the yaw angle of the upstream wind turbine can increase the overall power production. Although the upstream wind turbine cannot capture the optimum kinetic energy due to the change of yaw angle away from the wind direction, it reduces the impact on the downstream wind turbine by deflecting the wake direction by a certain degree. It is revealed from the present analysis that the control of the tilt angle, in addition to the control of the yaw angle of the upstream wind turbine, can raise the overall power production. Using higher yaw angles could increase the fatigue forces on the wind turbine blades due to



a) Power versus  $U^*$  and  $\theta^*$



b) Power versus  $U^*$  and  $\phi^*$



c) Power versus  $\theta^*$  and  $\phi^*$

Fig. 16. Response surface contours of the optimized tandem wind turbine layout.

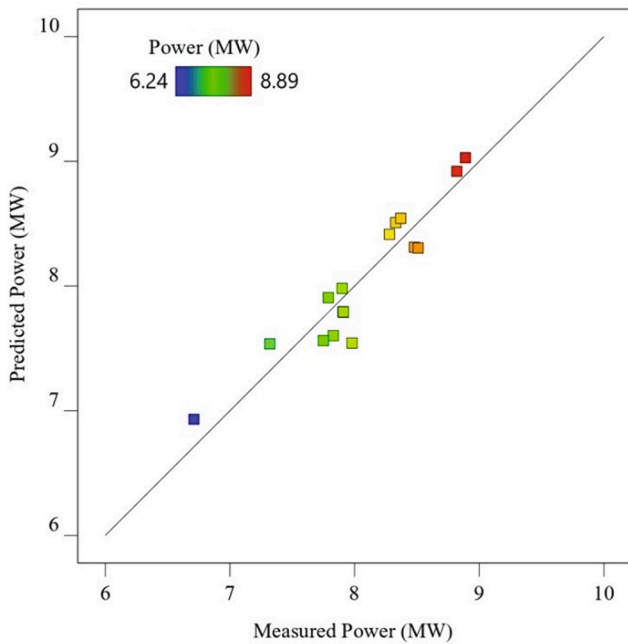


Fig. 17. Validation of the predicted wind farm power output with measured data.

additional flow disturbance and vortex generation over the yawed wind turbines. This study shows that a power increase of 17.1% is achieved by controlling both yaw and tilt angles. The power obtained from the present study is approximately 2.1% and 6.1% greater than those of Refs. [40] and [41], respectively. This observation is supported by calculating annual energy production (AEP) for different control methods, as shown in Fig. 19. Likewise, the AEP is increased by controlling both yaw and tilt angles, and an average increase of 3.7% is obtained in the present study compared to the previous wind farm wake-control studies of Howland et al. [43] and Fleming et al. [44].

5.2. Power generation improvement

Fig. 20 provides a combined power output generated from the upstream and downstream wind turbines using different control strategies. Both turbines have an average power capacity of 5 MW. Despite the upstream turbine generating at a full capacity, the power produced from

the downstream turbine is much lower in the case of 0° yaw and tilt angles. This results in an overall power output of 5.83 MW which is the lowest among the cases discussed in this study. Switching the upstream wind turbine slightly away from the wind direction reduces the effects of wakes applied on the downstream turbine, although the upstream wind turbine is not able to operate at a full capacity. In this study, it is found that setting the yaw angle of the upstream wind turbine to 30° can produce a combined power output of 7.9 MW. Switching the yaw angle to either positive or negative direction does not affect the power output as nearly identical power variations are obtained for positive and negative yaw angle cases in this study. The present study further reveals that controlling the tilt angle of the upstream wind turbine in addition to the yaw angle can produce more power output. In fact, it is shown that a combined power output of 8.29 MW is achieved when setting the yaw, and tilt angles of the upstream wind turbine to 30° and 24°, respectively. The output power is an increase of approximately 400 kW compared to setting the yaw angle alone.

6. Overall discussion

The comparison of the tangential force per unit length between the present simulation and the reference data suggests that the current ALM method predicts blade aerodynamic loads accurately, and this method can be reliably used for analysing and optimising blade design parameters. The current ALM method also captures the details of the blade tip loss correctly. As expected, the fully resolved LES model provides a great insight into the unsteady flow, turbulence, and wake behaviours around wind turbines. The instantaneous flow data shows that the downstream wind turbine is highly influenced by the wake structures from the upstream one, and a strong vortex generation is observed around and behind the downstream wind turbine.

As two wind turbines are arranged in an in-line configuration, the downstream turbine receives a non-uniform and turbulent inflow profile with a much lower velocity magnitude. Without a control strategy, the performance of the downstream turbine is significantly reduced. The wake from the upstream turbine should be controlled in order to reduce its impact on the downstream turbine. In this study it is shown that undesirable effects of wakes can be reduced by controlling the design parameters of the wind turbine such as the yaw angle and the tilt angle. Controlling the tilt angles deflects the wakes to an inclined upward direction, which leads to the wake structures generated from the upstream wind turbine partially passing over the downstream wind turbine. Using the proposed method, there is no need to place the turbines very far and as a result, more energy per area can be achieved.

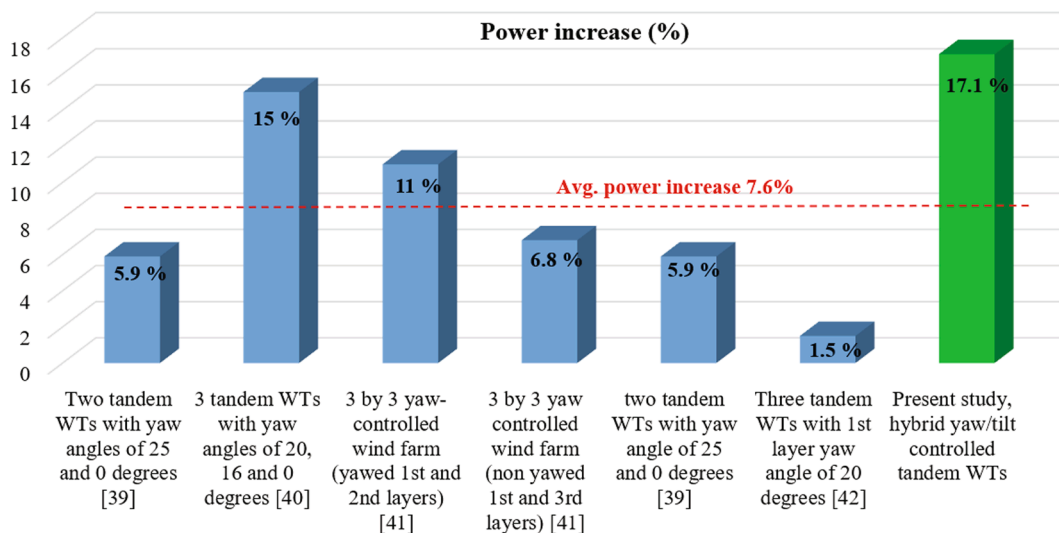


Fig. 18. Power production increase using different control methods at rated wind speed.

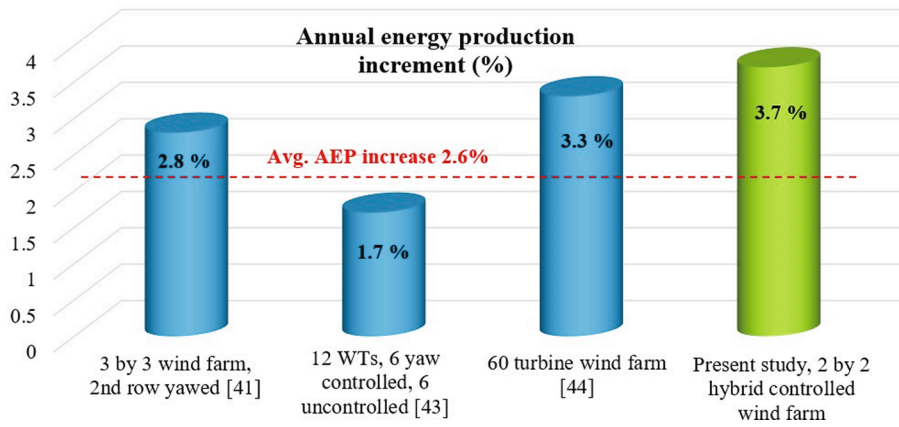


Fig. 19. Comparison of annual energy production increment using different control methods.

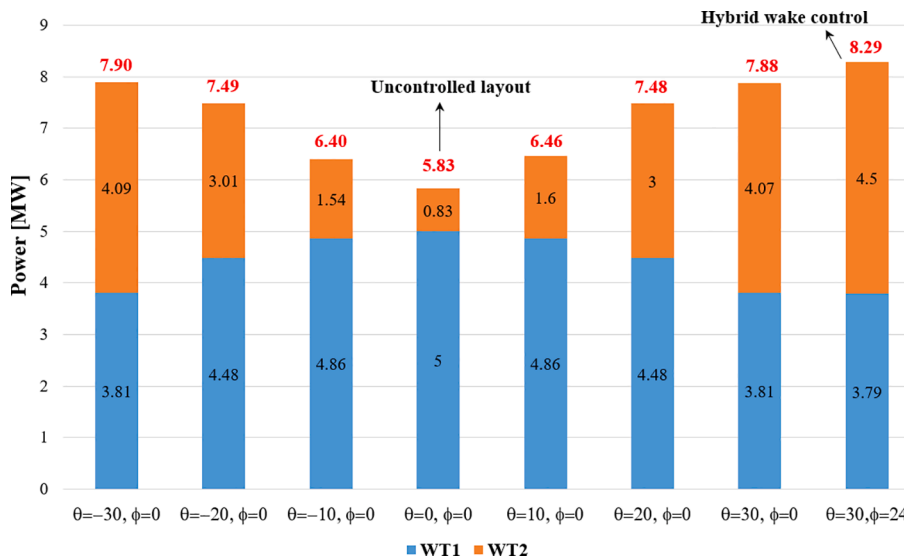


Fig. 20. Total output power of two turbines for different uncontrolled and controlled wind farm layouts at rated inflow velocity ( $U_{in} = 11.4$  m/s).

The proposed hybrid wake control strategy can be used in real horizontal-axis wind farms to increase the overall power generation. In complex offshore wind farm layouts, both yaw angle and tilt angle of the wind turbines can be optimised in real-time to react to fluctuations in the inflow wind, which is important for the AEP enhancement of large wind farms. These wake deflection angles must be controlled by sensitive sensors to the inflow wind directions.

### 7. Conclusion

Numerical investigations of two tandem wind turbines using a hybrid actuator line and the LES method are performed to analyse the aerodynamic flow behaviour and the power production from each turbine. The effects of yaw and tilt angle of the upstream wind turbine controlled and their effects on the flow and the power output are thoroughly investigated. In addition, an optimisation study is also performed to evaluate the optimum yaw and tilt angle of the upstream turbine to maximise the overall power output. The conclusions drawn from this study are listed below:

- It is concluded that hybrid control of the yaw and tilt angle of the upstream wind turbine results in an improvement of the overall performance of both wind turbines. The wake deflection occurs in both upward and side direction due to the change of yaw and tilt

angles, and the deflection is larger than controlling either yaw or tilt angle alone.

- An average power generation enhancement of 17.1% and an AEP improvement of 3.7% are achieved in this study by controlling both yaw and tilt angles.
- It is found that a combined power output of 8.29 MW is achieved when the yaw angle and the tilt angle of the upstream wind turbine are set to 30° and 24°, respectively, and this is an increase of about 400 kW compared to controlling the yaw angle alone.
- Changing the yaw angle of the upstream wind turbine away from the wind direction causes the change of direction and the twist of the wakes before reaching the downstream wind turbine. The wake deflection to the side is observed as a result.
- Changing the tilt angle of the upstream wind turbine leads to the wake deflection in the upward direction as some of the flow passes over the downstream wind turbine.

### CRedit authorship contribution statement

**M.E. Nakhchi:** Conceptualization, Methodology, Software, Formal analysis, Visualization, Writing – original draft. **S. Win Naung:** Conceptualization, Writing – review & editing, Validation, Investigation. **M. Rahmati:** Conceptualization, Writing – review & editing,

Resources, Funding acquisition, Project administration, Supervision.

### Data availability statement

All research data supporting this publication are directly available within this publication.

### Declaration of Competing Interest

The authors declare that they have no known competing financial interests or personal relationships that could have appeared to influence the work reported in this paper.

### Acknowledgement

The authors would like to acknowledge the financial support received from the Engineering Physics and Science Research Council of the UK (EPSRC EP/R010633/1).

### References

- [1] Adaramola M, Krogstad P-Å. Experimental investigation of wake effects on wind turbine performance. *Renewable Energy* 2011;36:2078–86.
- [2] Zilong T, Wei DX. Layout optimization of offshore wind farm considering spatially inhomogeneous wave loads. *Appl Energy* 2022;306:117947.
- [3] Dou B, Guala M, Lei L, Zeng P. Wake model for horizontal-axis wind and hydrokinetic turbines in yawed conditions. *Appl Energy* 2019;242:1383–95.
- [4] Sun H, Yang H. Study on an innovative three-dimensional wind turbine wake model. *Appl Energy* 2018;226:483–93.
- [5] Bastankhah M, Porté-Agel F. A new analytical model for wind-turbine wakes. *Renewable Energy* 2014;70:116–23.
- [6] Zhang T-T, Elsakka M, Huang W, Wang Z-G, Ingham DB, Ma L, et al. Winglet design for vertical axis wind turbines based on a design of experiment and CFD approach. *Energy Convers Manage* 2019;195:712–26.
- [7] Nilsson K, Ivanell S, Hansen KS, Mikkelsen R, Sørensen JN, Breton SP, et al. Large-eddy simulations of the Lillgrund wind farm. *Wind Energy* 2015;18:449–67.
- [8] Calaf M, Meneveau C, Meyers J. Large eddy simulation study of fully developed wind-turbine array boundary layers. *Phys Fluids* 2010;22:015110.
- [9] Naung SW, Nakhchi ME, Rahmati M. High-fidelity CFD simulations of two wind turbines in arrays using nonlinear frequency domain solution method. *Renewable Energy* 2021;174:984–1005.
- [10] Nakhchi M, Naung SW, Rahmati M. High-resolution direct numerical simulations of flow structure and aerodynamic performance of wind turbine airfoil at wide range of Reynolds numbers. *Energy* 2021;225:120261.
- [11] Baratchi F, Jeans T, Gerber A. Assessment of blade element actuator disk method for simulations of ducted tidal turbines. *Renewable Energy* 2020;154:290–304.
- [12] Ravensbergen M, Mohamed AB, Korobenko A. The actuator line method for wind turbine modelling applied in a variational multiscale framework. *Comput Fluids* 2020;201:104465.
- [13] Zhang J, Zhao X. A novel dynamic wind farm wake model based on deep learning. *Appl Energy* 2020;277:115552.
- [14] Witha B, Steinfeld G, Heinemann D. High-resolution offshore wake simulations with the LES model PALM. *Wind energy-impact of turbulence*. Springer 2014: 175–81.
- [15] Martínez-Tossas LA, Churchfield MJ, Leonardi S. Large eddy simulations of the flow past wind turbines: actuator line and disk modeling. *Wind Energy* 2015;18(6): 1047–60.
- [16] Sprague MA, Ananthan S, Vijayakumar G, Robinson M. ExaWind: A multifidelity modeling and simulation environment for wind energy. *Journal of Physics: Conference Series*. IOP Publishing 2020. p. 012071.
- [17] Maché M, Mouslim H, Mervoyer L, Medjroubi W, Stoevesand B, Peralta C. From meso-scale to micro scale LES modelling: Application by a wake effect study for an offshore wind farm. *ITM Web of Conferences EDP Sciences* 2014;2:01004.
- [18] Bartholomew P, Deskos G, Frantz RA, Schuch FN, Lamballais E, Laizet S. Xcompact3D: An open-source framework for solving turbulence problems on a Cartesian mesh. *SoftwareX*. 12 (2020) 100550.
- [19] Jha P, Churchfield M, Moriarty P, Schmitz S. Accuracy of state-of-the-art actuator-line modeling for wind turbine wakes. In: 51st AIAA Aerospace Sciences Meeting including the New Horizons Forum and Aerospace Exposition; 2013. p. 608.
- [20] Archer CL, Vassel-Be-Hagh A. Wake steering via yaw control in multi-turbine wind farms: recommendations based on large-eddy simulation. *Sustainable Energy Technol Assess* 2019;33:34–43.
- [21] Dar Z, Kar K, Sahni O, Chow JH. Windfarm power optimization using yaw angle control. *IEEE Trans Sustainable Energy* 2016;8:104–16.
- [22] Dilip D, Porté-Agel F. Wind turbine wake mitigation through blade pitch offset. *Energies* 2017;10:757.
- [23] Cossu C. Evaluation of tilt control for wind-turbine arrays in the atmospheric boundary layer. *Wind Energy Science* 2021;6:663–75.
- [24] Gebraad PM, Fleming PA, van Wingerden J-W. Comparison of actuation methods for wake control in wind plants. 2015 American Control Conference (ACC). IEEE2015. pp. 1695-701.
- [25] Nash R, Nouri R, Vassel-Be-Hagh A. Wind turbine wake control strategies: a review and concept proposal. *Energy Convers Manage* 245 (2021) 114581.
- [26] Yang X, Pakula M, Sotiropoulos F. Large-eddy simulation of a utility-scale wind farm in complex terrain. *Appl Energy* 2018;229:767–77.
- [27] Wang J, Bottasso CL, Campagnolo F. Wake redirection: comparison of analytical, numerical and experimental models. *Journal of Physics: Conference Series*. IOP Publishing 2016. p. 032064.
- [28] Weipao M, Chun L, Jun Y, Yang Y, Xiaoyun X. Numerical investigation of wake control strategies for maximizing the power generation of wind farm. *J Sol Energy Eng* 2016;138:034501.
- [29] Moreno SR, Pierrezan J, dos Santos Coelho L, Mariani VC. Multi-objective lightning search algorithm applied to wind farm layout optimization. *Energy* 2021;216: 119214.
- [30] Wang Y, Miao W, Ding Q, Li C, Xiang B. Numerical investigations on control strategies of wake deviation for large wind turbines in an offshore wind farm. *Ocean Eng* 2019;173:794–801.
- [31] Deskos G, Laizet S, Palacios R. WInc3D: a novel framework for turbulence-resolving simulations of wind farm wake interactions. *Wind Energy* 2020;23: 779–94.
- [32] Onel HC, Tuncer IH. Investigation of wind turbine wakes and wake recovery in a tandem configuration using actuator line model with LES. *Comput Fluids* 2021; 220:104872.
- [33] Pope SB, Pope SB. *Turbulent flows*. Cambridge university press 2000.
- [34] Sorensen JN, Shen WZ. Numerical modeling of wind turbine wakes. *J Fluids Eng* 2002;124:393–9.
- [35] Churchfield MJ, Schreck SJ, Martinez LA, Meneveau C, Spalart PR. An advanced actuator line method for wind energy applications and beyond. In: 35th Wind Energy Symposium; 2017. p. 1998.
- [36] Qian Y, Wang T, Yuan Y, Zhang Y. Comparative study on wind turbine wakes using a modified partially-averaged Navier-Stokes method and large eddy simulation. *Energy* 2020;206:118147.
- [37] Dose B, Rahimi H, Herráez I, Stoevesand B, Peinke J. Fluid-structure coupled computations of the NREL 5 MW wind turbine by means of CFD. *Renewable Energy* 2018;129:591–605.
- [38] Sedaghatzadeh N, Arjomandi M, Kelso R, Cazzolato B, Ghayesh MH. Modelling of wind turbine wake using large eddy simulation. *Renewable Energy* 2018;115: 1166–76.
- [39] Lee J, Son E, Hwang B, Lee S. Blade pitch angle control for aerodynamic performance optimization of a wind farm. *Renewable Energy* 2013;54:124–30.
- [40] Nouri R, Vassel-Be-Hagh A, Archer CL. The Coriolis force and the direction of rotation of the blades significantly affect the wake of wind turbines. *Appl Energy* 2020;277:115511.
- [41] van Zalk J, Behrens P. The spatial extent of renewable and non-renewable power generation: A review and meta-analysis of power densities and their application in the US. *Energy Policy* 2018;123:83–91.
- [42] Wang J, Foley S, Nanos E, Yu T, Campagnolo F, Bottasso CL, et al. Numerical and experimental study of wake redirection techniques in a boundary layer wind tunnel. *Journal of Physics: Conference Series*. IOP Publishing 2017. p. 012048.
- [43] Howland MF, Lele SK, Dabiri JO. Wind farm power optimization through wake steering. *Proc Natl Acad Sci* 2019;116:14495–500.
- [44] Fleming PA, Ning A, Gebraad PM, Dykes K. Wind plant system engineering through optimization of layout and yaw control. *Wind Energy* 2016;19:329–44.